Gierut, Wood et al. Supplementary Figures

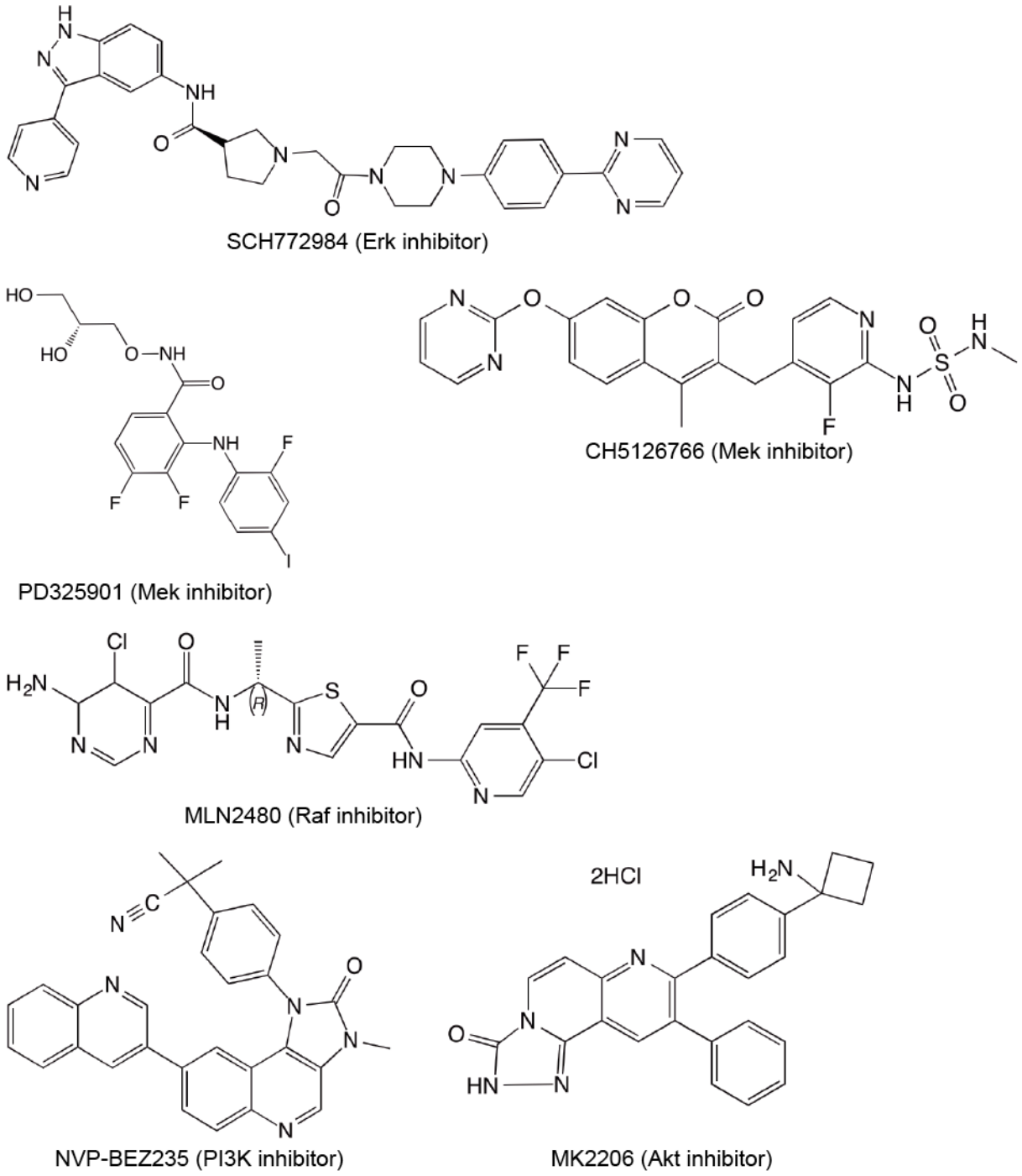

Fig. S1. Chemical structures of phosphoprotein signaling inhibitors.

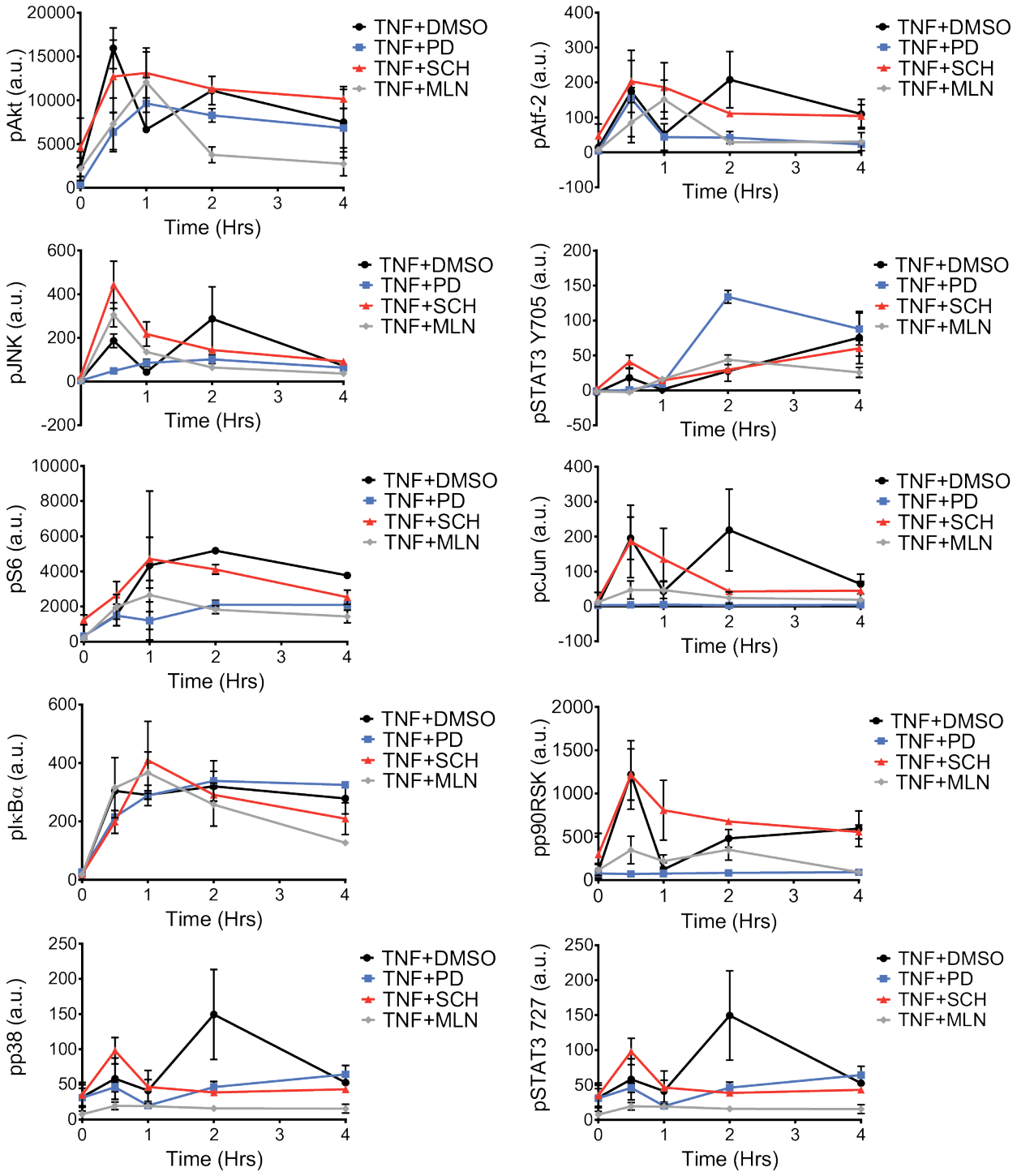

Fig. S2. MAPK pathway inhibitors alter the TNF-α-induced flux through multiple cellular signaling pathways (*N*=3-5 per time point; mean±SE). Mice were pretreated (as described in Materials and Methods) with DMSO (as a vehicle control), the MEK inhibitor PD325901 (PD), the ERK inhibitor SCH772984 (SCH), or the RAF inhibitor MLN2480 (MLN), as indicated, before being treated with TNF-α for the indicated times. Intestinal epithelia from the mice were then analyzed by Bio-Plex to determine the relative abundances of the indicated phosphoproteins. Data are means ± SEM of three to five animals per time point.

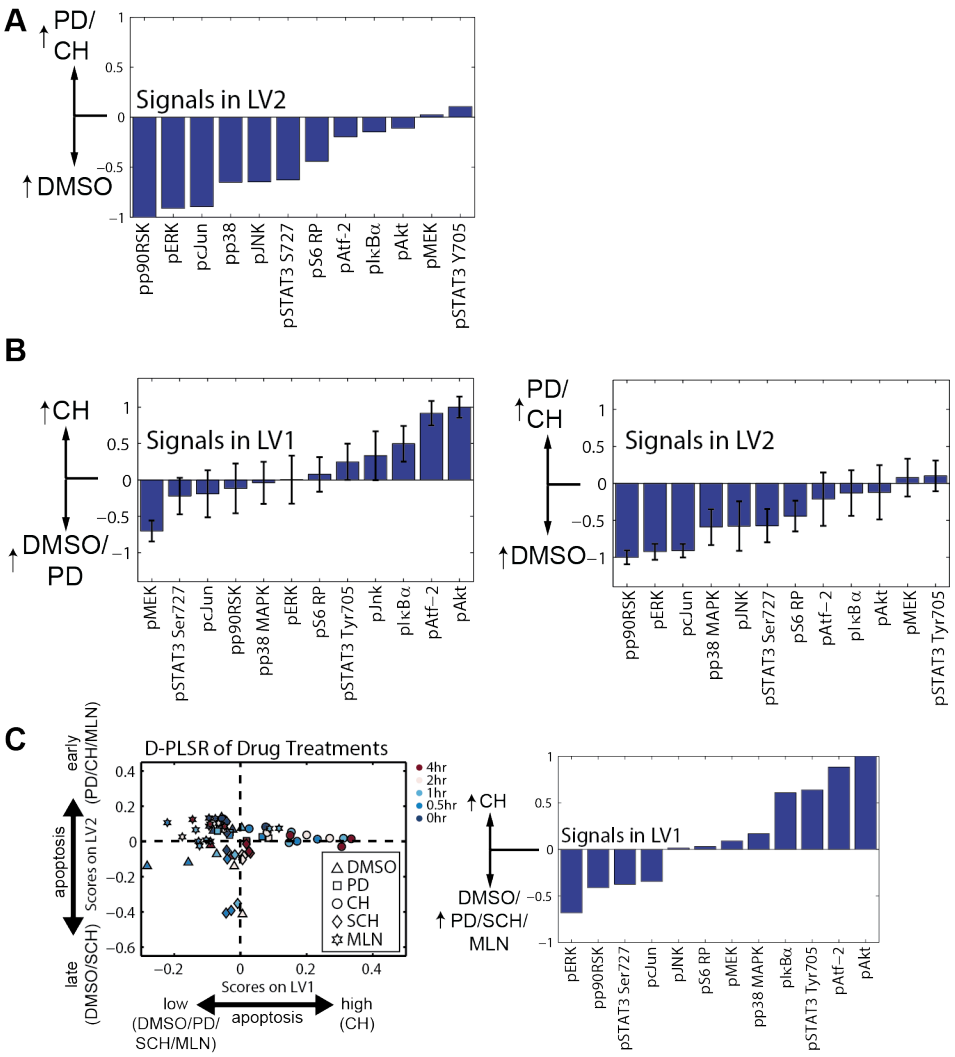

Fig. S3. D-PLSR analysis of the phosphoprotein signaling network. (**A**) Signals in LV2 separating DMSO-treated samples from CH5126766- and PD325901-treated samples in the scores plot. **(B)** Means±SD of signals in LV1 and LV2 from the three-condition model. SD was computed with a Monte-Carlo sub-sampling of the dataset used in Fig. 4A. **(C)** D-PLSR regression model constructed using the DMSO, PD, CH, SCH, and MLN conditions shows a scores plot and LV1 values that are similar to those shown in Fig. 4A.

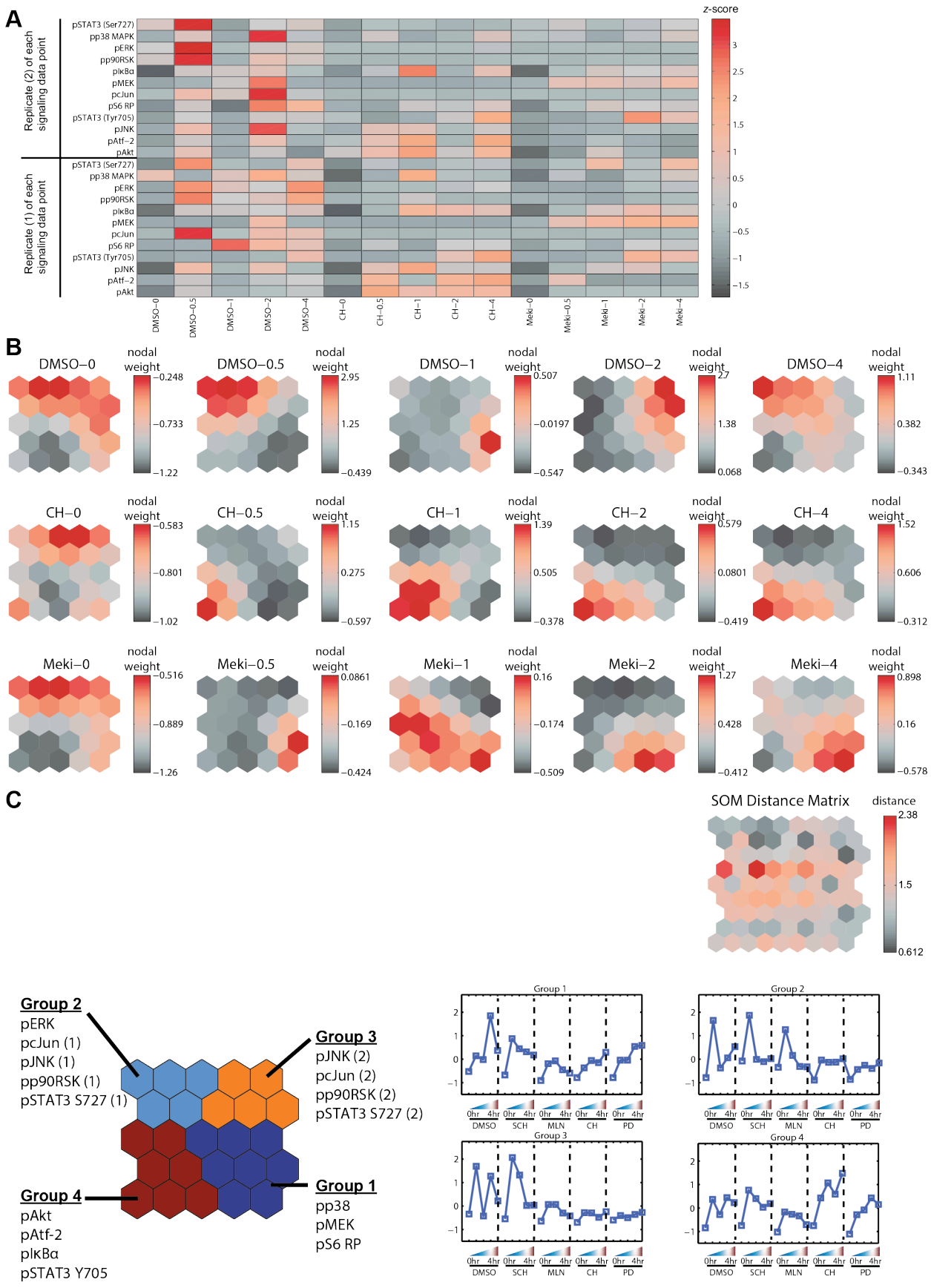
A
z-score
Replicate (2) of each signaling data point
Replicate (1) of each signaling data point
pSTAT3 (Ser727)
pp38 MAPK
pERK
pp90RSK
pIκBα
pMEK
pcJun
pS6 RP
pSTAT3 (Tyr705)
pJNK
pAtf−2
pAkt
DMSO−0
DMSO−0.5
DMSO−1
DMSO−2
DMSO−4
CH−0
CH−0.5
CH−1
CH−2
CH−4
Meki−0
Meki−0.5
Meki−1
Meki−2
Meki−4
B
nodal weight
C
SOM Distance Matrix
distance
Group 2
pERK
pcJun (1)
pJNK (1)
pp90RSK (1)
pSTAT3 S727 (1)
Group 3
pJNK (2)
pcJun (2)
pp90RSK (2)
pSTAT3 S727 (2)
Group 4
pAkt
pAtf-2
pIκBα
pSTAT3 Y705
Group 1
pp38
pMEK
pS6 RP
Group 1
Group 2
Group 3
Group 4
0hr 4hr
DMSO
SCH
MLN
CH
PD

Fig. S4. SOM analysis of the phosphoprotein signaling network. (A) Replicates (1) and (2) of each signaling data point presented to the SOM in Fig. 4C for nodal training. **(B)** Component planes illustrate the activation of regions of the map that correspond to different phosphoprotein signaling nodes, as illustrated in Fig 4C. **(C)** SOMs generated using the DMSO, PD, CH, SCH, and MLN conditions.

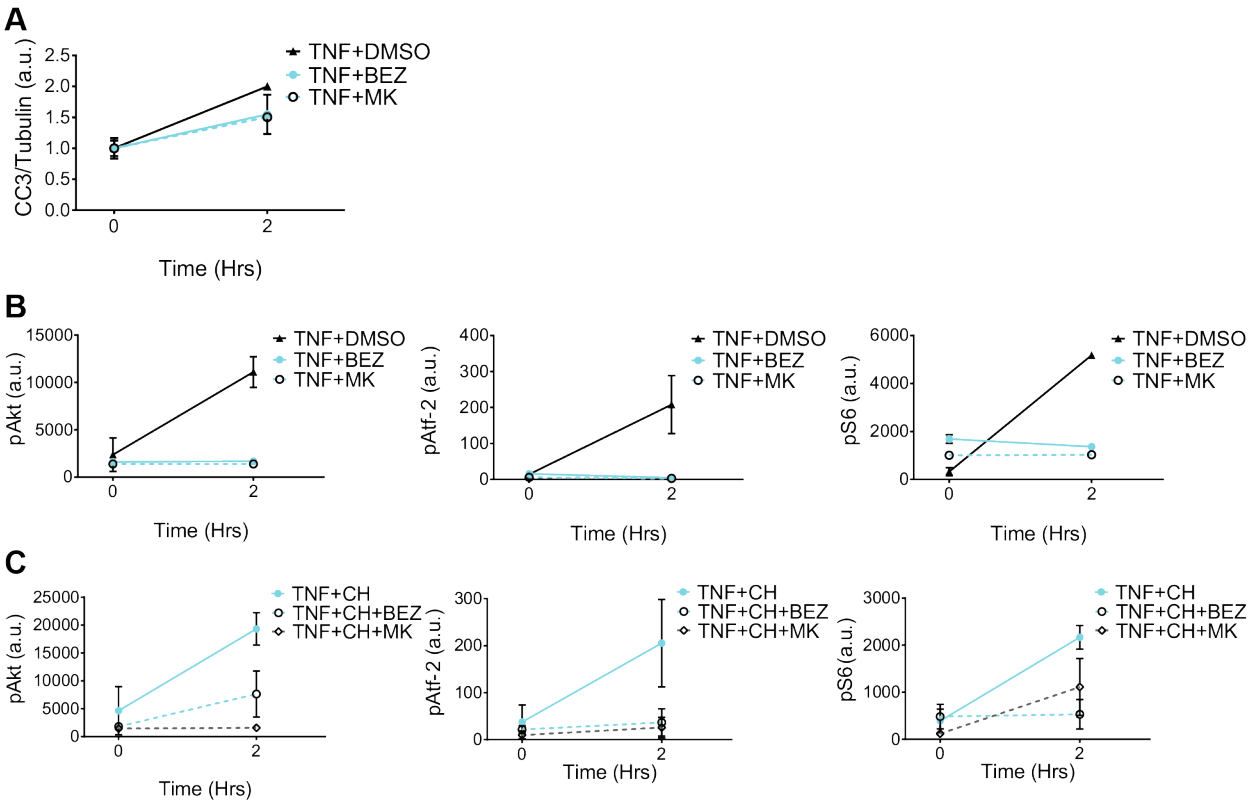

Fig. S5. Influence of the Akt pathway inhibitors (BEZ235 and MK2206) on CC3 abundance and phosphoprotein signaling. (A and B) Mice were pretreated with DMSO, the PI3K inhibitor NVP-BEZ235 (BEZ), or the Akt inhibitor MK2206 (MK), as indicated, before being treated with TNF-α for the indicated times. Intestinal epithelia from the mice were then analyzed by Bio-Plex to determine (A) the relative abundance of cleaved caspase-3 (CC3), normalized to that of tubulin, and (B) the relative abundances of the indicated phosphoproteins. Data in (A) and (B) are means ± SEM of two or three experiments per time point. **(C)** Mice were pretreated with the MEK inhibitor CH5126766 (CH) in the presence or absence of the PI3K inhibitor NVP-BEZ235 (BEZ) or the Akt inhibitor MK2206 (MK), as indicated, before being treated with TNF-α for the indicated times. Intestinal epithelia from the mice were then analyzed by Bio-Plex to determine the relative abundances of the indicated phosphoproteins. Data are means ± SEM of three to five experiments per time point.